

High-Q Micromachined Silver Passives and Filters

Mina Rais-Zadeh¹, Paul A. Kohl², and Farrokh Ayazi¹

¹School of Electrical and Computer Engineering, ²School of Chemical and Biomolecular Engineering
Georgia Institute of Technology
85 5th street NW, Atlanta, GA, 30308, USA

Abstract

This paper presents high aspect-ratio silver (Ag) micromachining for implementation of very high quality factor (Q) tunable and fixed passives, and low insertion loss bandpass LC filters. A combination of low-loss substrate and highest conductivity metal is used to achieve record high Q and low insertion loss (IL) at radio frequencies.

Introduction

MEMS-based RF components are leading candidates for cellular front-end modules that need to support an increasing number of frequency bands and communication standards. Currently, most of the high-Q bandpass filters used in cellular modules are realized using off-chip, acoustic-resonant components, such as SAW devices. While SAW filters offer very low insertion loss (IL) and high quality factor (Q), they cannot be tuned, and therefore many transmit and receive SAW filters are needed to cover multiple frequency bands. Also, off-chip components must interface with integrated electronics at the board level, which introduces additional loss and creates a bottleneck to miniaturization of these modules. Integrated single chip solutions to cellular modules are therefore desirable. Tunable MEMS LC filters can be prime candidates for multi-band cellular application if they meet the desired band specification in terms of insertion loss, out of band rejection, and Q. To increase the Q of an LC filter while maintaining low insertion loss, high Q tunable capacitors and inductors are needed. In this work, high aspect-ratio silver (Ag) micromachining is used to create lateral tunable capacitors, record high-Q inductors, and bandpass filters. The loss of silicon (Si) substrate is eliminated by using micromachining techniques. Using the presented CMOS-compatible fabrication process, a third order elliptic LC filter is fabricated, which exhibits an IL of 0.9dB at 1.2GHz. Wafer-level polymer packaging of the filter did not cause any additional loss.

Fabrication

The fabrication process of tunable and fixed silver passives is shown in Fig. 1. To reduce the high frequency loss of CMOS grade Si substrate (10-20Ω.cm), the substrate is first passivated with a 20μm thick low-loss polymer. We chose

Avatrel from Promerus for this purpose because of its low permittivity and loss tangent [1]. Next, a 2μm thick routing layer of titanium/silver is evaporated and patterned. The sacrificial silicon dioxide layer is then deposited at 250°C (the highest processing temperature) and patterned. Thick silver (40μm) is then electroplated into NR4-8000P negative-tone photoresist from Futurrex as the electroplating mold [2]. The loss of Si substrate is then eliminated by selective backside etching of Si underneath the passives, leaving behind a thin diaphragm of Avatrel polymer. Finally, devices are released in buffer oxide etch. The inductors as well as fixed and tunable capacitors are simultaneously fabricated using this process.

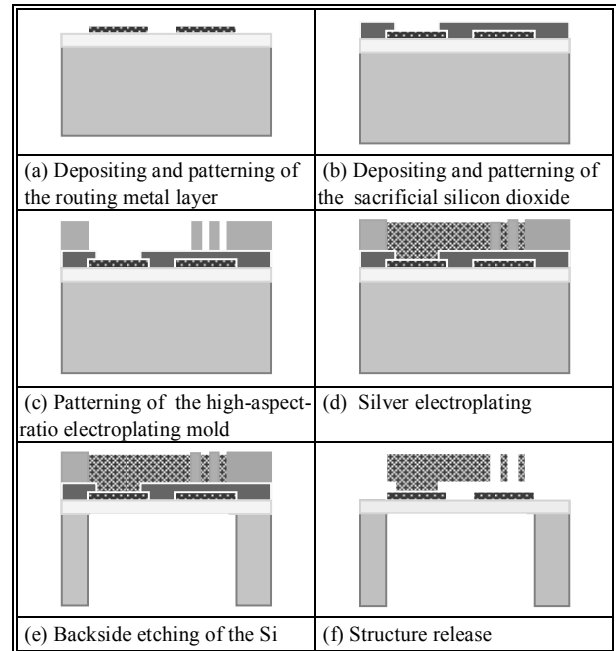


Fig. 1. Fabrication process flow of MEMS silver passives.

Results and Discussion

The Ag passives have very small series resistance due to the high conductivity of electroplated silver [3], and thus can exhibit very high Q. Therefore, special care must be taken in measuring the Q. On-wafer S-parameter measurements of the fabricated devices have been carried out using *hp8510C* vector network analyzer and Cascade GSG infinity (I-50) microprobes. Accurate measurement of Q's in excess of 80

calls for a very thorough calibration. Herein, calibration is done using both SOLT and LRRM calibration procedure and the pad parasitics were not de-embedded to avoid over estimation of Q. Also, to ensure repeatability in the measurements, the high Q passives are measured several times, and each time the calibration was redone. The deviation of the measurement values is within 10% for Q's in excess of 100.

A. Tunable Capacitors

Fig. 2 shows the SEM view of a high aspect-ratio 40μm thick silver tunable lateral capacitor. Dual gap actuation scheme has been chosen to get the highest tuning range. Fig. 3 is the extracted Q of this capacitor, showing Q>100 up to 3GHz and self resonance frequency (SRF) of above 6GHz. The Q and the capacitance (C) are extracted from the measured S-parameter using the following formulas:

$$Q = \frac{\text{Im}(Y_{11})}{\text{Re}(Y_{11})}, \text{ and } C = \frac{\text{Im}(Y_{11})}{\omega(\text{Re}(Y_{11}) - 1)} \quad (1)$$

where, ω is the angular frequency. The actuation gap of this capacitor is 3 times the sense gap, and therefore the tuning range of this capacitor is ideally infinite with the application of 150V. The capacitor exhibits a tuning of 3.3:1 with the application of 100V. The C-V tuning curve of this capacitor is shown in Fig. 4.

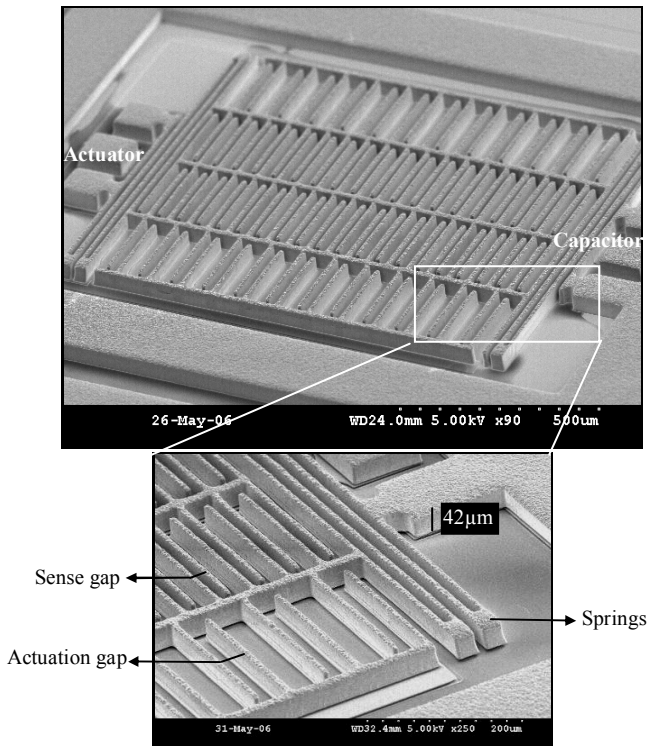


Fig. 2. SEM view of a 40μm thick tunable Ag capacitor.

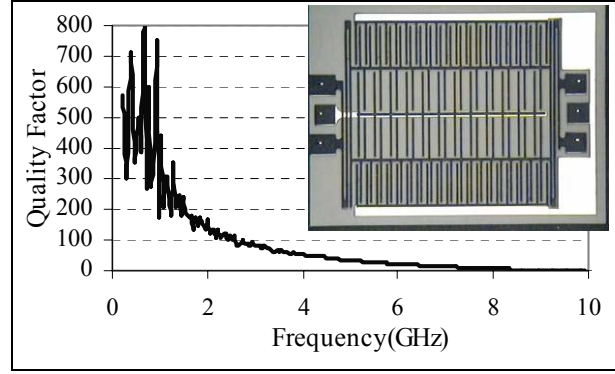


Fig. 3. Measured Q of a 0.4pF tunable capacitor fabricated on Avarel diaphragm with a micrograph of the capacitor.

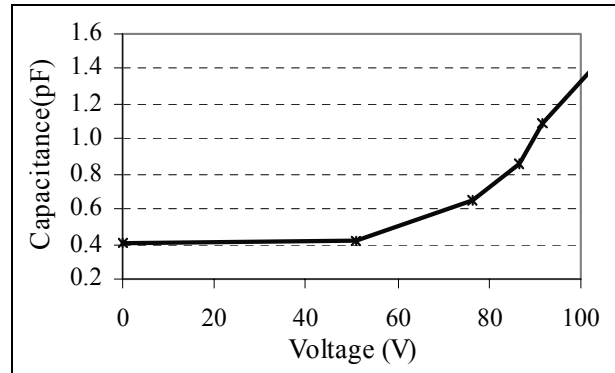


Fig. 4. C-V tuning curve of the silver capacitor shown in Fig. 3.

Fig. 5 shows the tuning curve of another dual gap capacitor of 0.66pF, which has a smaller actuation gap (20μm), longer fingers, and same sense gap (10μm). This capacitor is tuned by 130% with a tuning voltage of 58V.

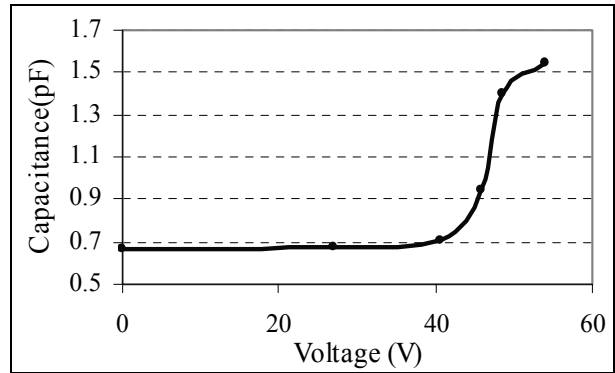


Fig. 5. C-V tuning curve of a 0.66pF silver capacitor.

Tuning voltages of these capacitors are high due to the conservative design of the gap size, and can be reduced by decreasing the actuation gap and the spring width. Also, the high frequency Q of these capacitors is low because of the series parasitic inductance of the folded springs, which significantly lowers the SRF. Use of non-folded springs would considerably improve the high frequency behavior of these tunable capacitors.

B. High-Q Inductors

Due to extreme reduction of both the metal loss and the substrate loss, fabricated inductors have exceptionally high Q. Fig. 6 shows the SEM view of a 40 μm thick 0.6nH inductor that exhibits a high Q of >200 at 8GHz. The S-parameters of this inductor have been simulated in Sonnet, using Sonnet thick metal model. The simulated Q validates the accuracy of the high measured Q (Fig. 7).

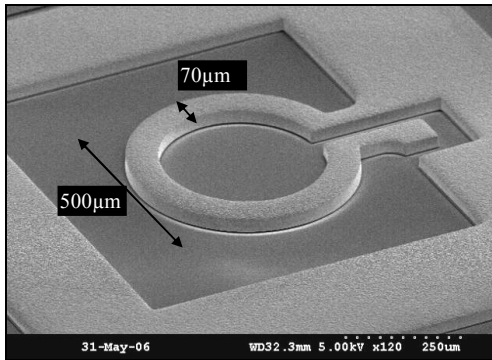


Fig. 6. SEM view of a 40 μm thick, 0.6nH silver inductor.

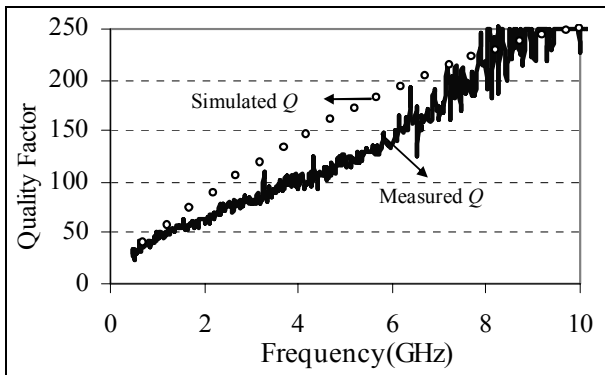


Fig. 7. Measured and simulated Q of the inductor in Fig. 6.

A fabricated 1nH inductor shows a very high Q of >150 at 8-23GHz frequency range (Fig. 8). To our best knowledge, this is the highest measured embedded Q for spiral inductors at such high frequency.

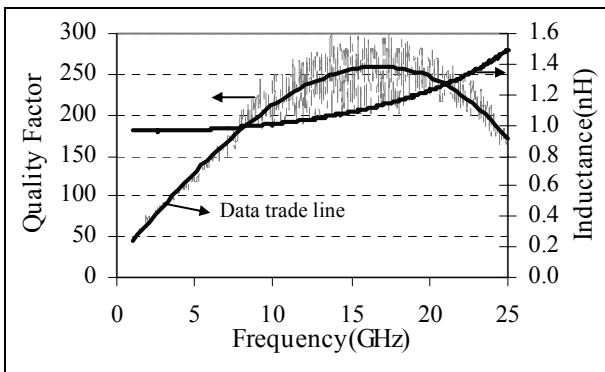


Fig. 8. Measured Q and inductance of a one-turn 1nH inductor on Avatrel diaphragm, showing Q in excess of 180 in 8-23GHz range.

To explore the effect of using silver on reduction of the metal loss, an eight-turn 32nH inductor was fabricated. The fabricated inductor exhibits a high Q of 35 at 1.2GHz, with a SRF of larger than 3GHz (Fig. 9). Fig. 10 shows (a) the SEM view of this inductor along with (b) the micrograph of the inductor taken from backside of the wafer showing the device on Avatrel diaphragm.

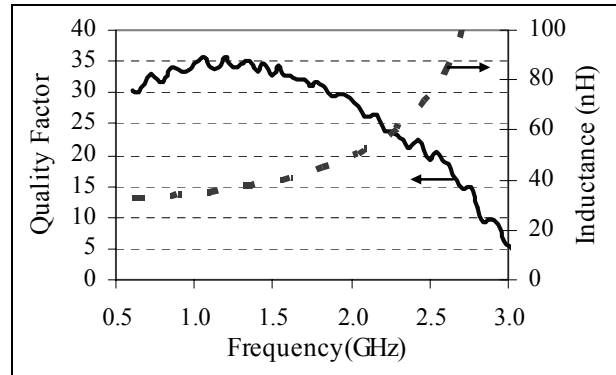


Fig. 9. Measured Q and inductance of a 32nH silver inductor.

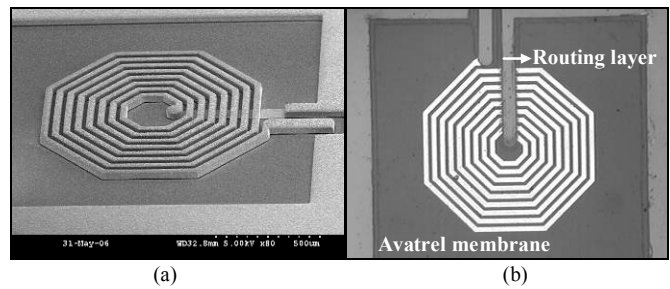


Fig. 10. (a) SEM view of a 32nH inductor, (b) micrograph of the inductor taken from backside of the wafer.

C. Bandpass Filter

A third-order elliptic LC filter has been designed and fabricated using this process. The filter is designed to have 300MHz bandwidth (BW) at the center frequency of 1GHz. Fig. 11 depicts the measured S_{21} of two identical filters, one fabricated on Avatrel diaphragm (Si was removed), and the other fabricated on the passivated CMOS grade Si substrate (Si was not removed). The fabricated filter on Avatrel diaphragm exhibits a very low IL of 0.9dB at 1.2GHz when terminated to 50 Ω , which corresponds to an inductor Q of 60 and a capacitor Q of 100 at 1.2 GHz. The identical filter on Si has an IL of 3.6dB. The small deviation of the center frequency from the designed value is due to imprecise thickness of the sacrificial silicon dioxide layer. The SEM view of the fabricated filter is shown in Fig. 12. With a capacitive gap of 3.5 μm , the LC filter occupies 3mm \times 3mm of die area (Fig. 12).

Reducing the capacitive gap thickness would significantly reduce the size of each capacitor and consecutively the filter.

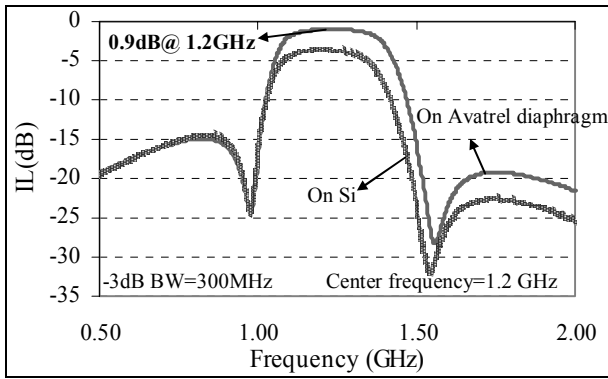


Fig. 11. Measured S_{21} of a 3rd order elliptic filter fabricated on Avatrel diaphragm and Si, showing an insertion loss of 0.9dB on Avatrel and 3.6dB on CMOS grade Si.

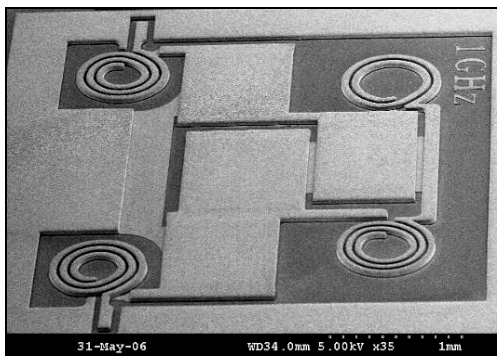


Fig. 12. SEM view of the 3rd order elliptic filter.

The fabricated filter on Si substrate was subsequently packaged using the wafer-level thermally-released polymer packaging technique described in [4]. The measured frequency responses of two identical filters, one packaged and one unpackaged are shown in Fig. 13. The packaged filter does not show any additional insertion loss. SEM view of the packaged filter is shown in Fig. 14.

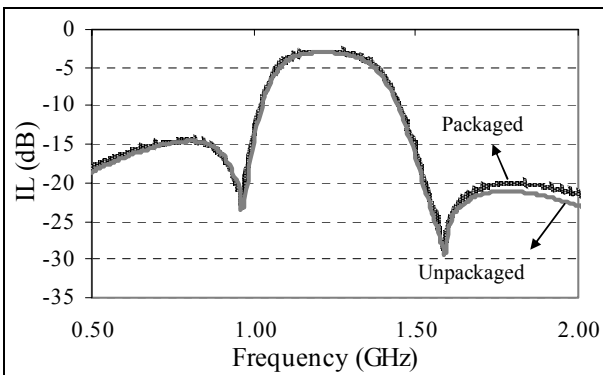


Fig. 13. Measured S_{21} of two identical filters fabricated on the same die, one packaged, showing no additional loss for the packaged filter.

Quality factor of individual fixed components used in the filter of Fig. 12 were measured on test structures. A 3.2nH inductor and a 3.8pF capacitor exhibit Q of 60, and 102 at 1.2GHz, respectively (Fig. 15). Smaller capacitors and larger inductors

used in this filter have higher Q at 1.2GHz, and thus this is the lower bound of individual Q. Performance of the silver passives and filters can be further improved by increasing the thickness of the routing metal layer.

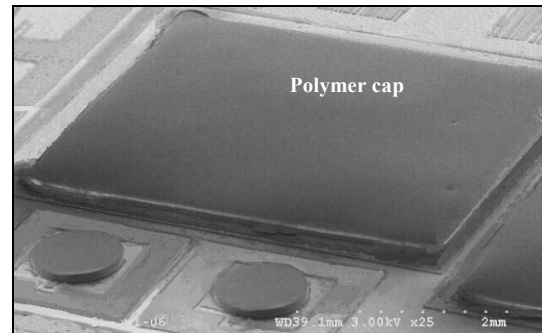


Fig. 14. SEM view of the packaged filter.

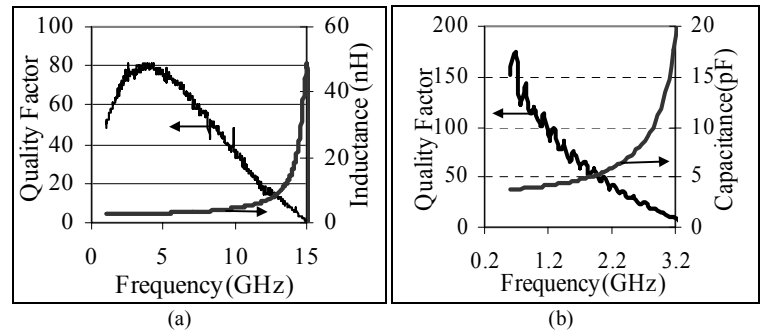


Fig. 15. Measured characteristic of individual filter components. (a) A 3.2nH inductor, and (b) a 3.8pF capacitor.

Conclusion

A new implementation of high-Q tunable and fixed passives was presented. High aspect-ratio silver technology was used to improve the metal loss of passives at RF frequency. A 0.4pF tunable capacitor shows an embedded $Q > 250$ at 1GHz, and a tuning of 2.3:1. A 1nH inductor fabricated using the same technique exhibits $Q > 150$ in 8-23GHz range. A 3rd order elliptic filter shows an IL of 0.9dB at 1.2GHz. Wafer-level polymer packaging of the filter did not cause any additional loss.

References

- [1] M. Rais-Zadeh, and F. Ayazi, "Characterization of high-Q spiral inductors on thick insulator-on-silicon," *Journal of Micromechanics and Microengineering*, vol. 15, pp. 2105-2112, Sept. 2005.
- [2] M. Raieszadeh, S. W. Yoon, P. Monajemi, J. Laskar, and F. Ayazi, "High-Q integrated inductors on etched Si islands," *Proc. IEEE Micro Electro Mechanical Systems Conference (MEMS 2005)*, Miami, FL, Jan. 2005, pp. 199-202.
- [3] R. Manepalli, F. Stepniak, S. A. Bidstrup-Allen, and P. A. Kohl, "Silver metallization for advanced interconnects," *IEEE Trans. Advanced Packaging*, vol. 22, no.1, Feb. 1999, pp. 4-8.
- [4] P. Monajemi, P. Joseph, P. Kohl, and F. Ayazi, "A Low Cost Wafer-Level MEMS Packaging Technology," *Proc. IEEE Micro Electro Mechanical Systems Conference*, Miami, FL, Jan. 2005, pp. 634-637.